ON THE SUBJECT OF ELECTRIC SUBMERGED-ARC WELDING

V.G. KUZMENKO
E.O. Paton Electric Welding Institute, NASU, Kiev, Ukraine

Results of investigation of the nature of flux melting in electric submerged-arc welding with slag bubble formation are described. It is established that the flux melts without formation of a slag bubble by the gas-plasma flows of the arc in the convective heat exchange mode. These conclusions are confirmed by visual observations of electric arc running under flux, using a procedure specially developed for this purpose. Moreover, an extended plume of liquid slag forms in the post-arc zone, which is separated from the weld metal by a wedge-like layer of solid slag. The process of slag crust formation is also due to high heat-insulating properties of welding fluxes.

Keywords: *electric submerged-arc welding, slag bubble, thermophysics, flux heat conductivity, hydrodynamics, visual observation of arcing, process diagram*

Some postulates of this work are given in papers, published in the way of discussion in «Avtomaticheskaya Svarka» [1, 2] and «Svarochnoe Proizvodstvo» [3, 4] journals.

The concept of electric arc welding (Figure 1) was formed in the middle of the XX century [5, 6], proceeding from the data of arcing zone examination by X-rays, based on which the authors came to the conclusion that the arc functions in the atmosphere of a slag bubble, forming from the melting flux.

Several remarks can be made on the investigation procedure: absence of preliminary identification of the differences between liquid slag and solid flux in the pre-arc zone, fragmentary nature of the filmed material, because of the short time of filming exposure (0.02 s), complexity of identifying the thin slag shell against the background of flux grains, and other factors, casting doubt on the obviousness of the above conclusions.

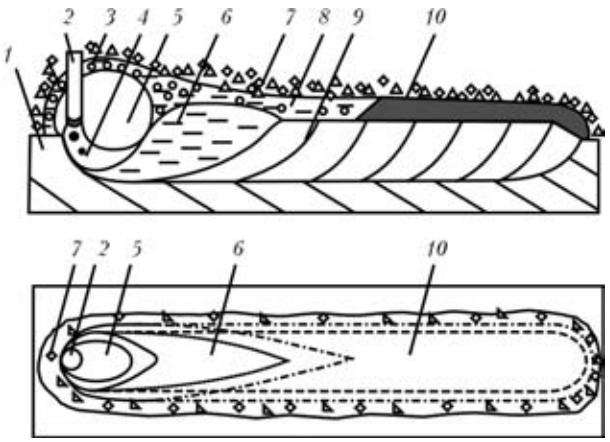

Figure 1. Schematic of the process of electric submerged-arc welding according to the current concepts: *1* — base metal; *2* — electrode wire; *3* — slag bubble; *4* — arcing zone; *5* — crater; *6* — weld pool; *7* — flux; *8* — liquid slag; *9* — weld; *10* — slag crust

A feature of the electric arc column is its ability to push out of its space the solid and liquid components that is accompanied by formation of a cavity in the flux grain bulk. It was this cavity, possibly, that was recorded on the obtained rentgenograms. The question is, whether there is enough time for the liquid slag interlayer creating a closed shell around the arc, to form during welding in the flux volume ahead of the arc? This question is essential for assessment of the mechanism of weld pool metal protection from the influence of the components of the ambient air atmosphere.

Similar research was performed also by other authors [7–9]. So in [7] the X-ray image was sent to electron-optical tube, thus allowing the arcing process to be observed in its dynamics and electrode metal transfer to be studied both in manual electrode and flux-cored wire, and in submerged-arc welding. Nonetheless, based on the results of the performed research it is impossible to unambiguously determine the presence of slag shell in submerged-arc welding, particularly in the pre-arc zone. In order to determine the actual situation, we have conducted studies, including both theoretical calculations and special experiments.

The slag bubble in the case of its actual existence can be regarded as some dynamically stable formation, insulating the arcing zone from ambient air, and also having the function of liquid slag supplier, which is consumed for weld pool shielding. Slag bubble should be able to restore itself, and during welding should provide transfer of sufficient quantity of heat from the arc to solid flux beyond the slag shell. Using the known expression [10, 11], the time for heat transfer through the front wall of slag shell was determined, which was required to bring a certain amount of solid flux to melting temperature:

$$\tau = \frac{Q\delta}{\lambda(t_{st2} - t_{st1})F},$$

where Q is the heat that should be consumed for heating a certain amount of flux up to melting temperature; δ is the thickness of slag bubble shell; λ is the coef-

ficient of slag heat conductivity; $t_{st1} - t_{st2}$ is the temperature difference on the surfaces inside and outside the shell, respectively; F is the area of shell surface.

Such thermophysical properties of slags as specific heat capacity, density and heat conductivity, assumed by us for calculations, were taken from published sources [12–24]. Values of the thickness of slag bubble wall and temperature on its inner surface were assigned, and the temperature on the bubble outer surface was taken equal to flux melting temperature (1200 °C). For slag bubble wall inner surface the temperature was taken to be approximately equal to slag boiling temperature (3000 °C).

As shown by calculations, values of the speed of slag bubble shell restoration ahead of the moving arc (speed of shifting of flux melting isotherm) (Figure 2) are 3–4 times lower than the actual welding speed that calls in question the probability of formation of a liquid slag wall ahead of the arc in the respective welding process.

Existence of a slag bubble in submerged-arc welding is possible only in the presence of a sufficiently fine equilibrium between gas pressure in its volume, on the one hand, and interphase (surface) slag tension and flux mass, on the other, as well as at the absence of strong disturbance factors in the zone of slag bubble formation. Let us consider this in the real welding process as far as possible.

In welding the arc applies strong pressure to the edge of melting plate and weld pool liquid metal that is caused by its strong gas-plasma flows, the velocity of which, by various data, is equal from 75 to 2200 m/s [25–34]. As a result of reflection from the melting edge of metal being welded, these flows change their direction to the side opposite to arc motion. Here, a considerable portion of weld pool liquid metal is pressed out and a crater forms. Gas-plasma flows drive away liquid slag even more intensively, as its density is much lower than that of metal. This is confirmed by the data earlier obtained by us by indication method [1, 3] on the nature of metal and slag displacement after welding. Metal and slag acquire the maximum speed exactly at the first moment of contact with the arc. Presence of strong disturbance of metal and slag resulting from the arc impact prevents formation of the slag bubble in the considered welding process in connection with shifting of its supporting zone at a high speed that is confirmed by the data of investigations of liquid slag distribution along the weld pool obtained by ejection of its contents into a special collector with uniformly located sections [1, 3]. Figure 3 shows slag distribution along the weld pool at application of three standard fluxes of AN-60, AN-26S and AN-15M grades obtained by the above procedure. As follows from experimental results, welding slag is nonuniformly distributed along the welding zone. A considerable part of it is driven by the arc into the weld pool tail zone, and a marked

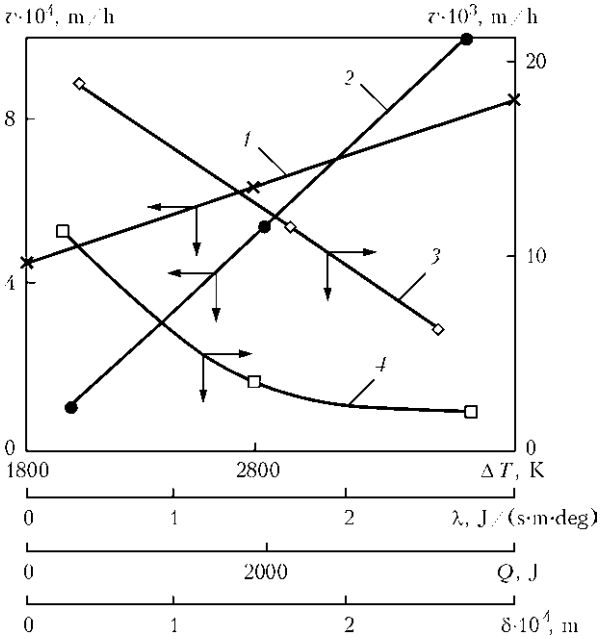

Figure 2. Change of the speed of restoration of slag bubble shell v in the pre-arc zone in electric submerged-arc welding depending on thermophysical characteristics: *1* — temperature gradient $\Delta T(t_{st2} - t_{st1})$ (shell thickness δ = 2 mm; heat capacity of slag of 1 × 1 × 2 mm volume Q = 1177 J; λ = 1.5 J/(s·m·deg)); *2* — coefficient of slag heat conductivity λ (δ = 2 mm; Q = 1177 J of slag of indicated volume; ΔT = 2300 K); *3* — heat capacity Q of slag of indicated volume (δ = 2 mm; λ = 2 J/(s·m·deg); ΔT = = 2300 K); *4* — thickness of slag bubble shell δ (Q = 1177 J of slag of indicated volume; ΔT =2300 K; λ = 1.5 J/(s·m·deg)

tendency to lowering of liquid slag mass towards the melting metal edge is found in its head part. To obtain a clearer picture, similar experiments were conducted to monitor the presence of liquid slag on weld pool front edge, using lower arc voltage (21 V) that allowed limiting the volume of melting flux, which was masking the experimental results. In Figure 4 it is

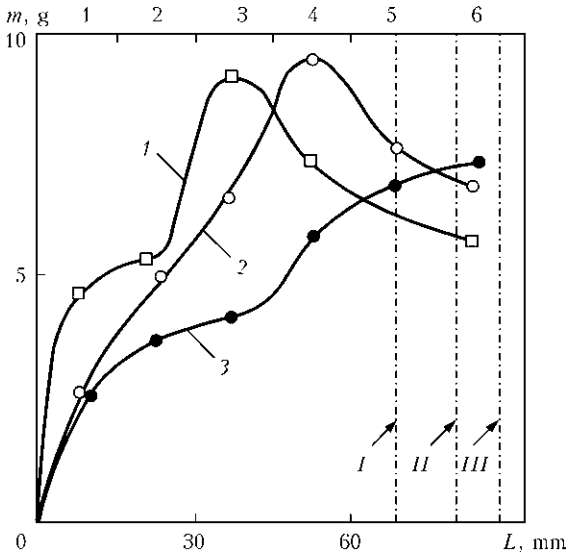

Figure 3. Distribution of mass m of slag along length L of weld pool in electric submerged-arc arc welding with fluxes of AN-60 (*1*), AN-26S (*2*) and AN-15M (*3*) grades established by turning over its contents into a collector with pockets 1–6, uniformly placed along the weld pool, and subsequent weighing of slag (arrows are weld pool boundaries at application of the above flux grades in the sequence corresponding to designated row *I–III*)

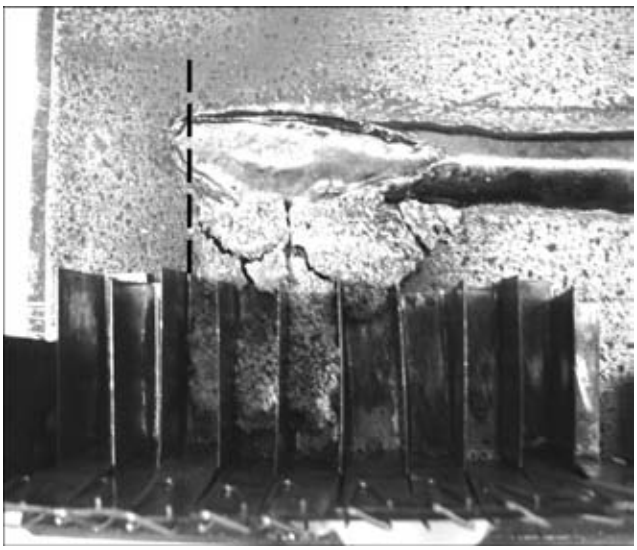

Figure 4. Distribution of molten slag along the weld pool in electric arc welding after removal of unmolten flux and slag crust (experimental phase)

clearly seen that liquid slag is absent on the edge in front of weld pool melting metal (marked by a dashed line), and it is not found also on a certain portion of weld pool head part, where the arc runs. This is confirmed by curves plotted by the data of weighing the contents of each of the collector pockets (Figure 5, *a*). Thus, investigations of slag distribution along the weld pool did not demonstrate its presence on the weld pool front edge that, essentially, eliminates the possibility of slag bubble existence in electric submerged-arc welding.

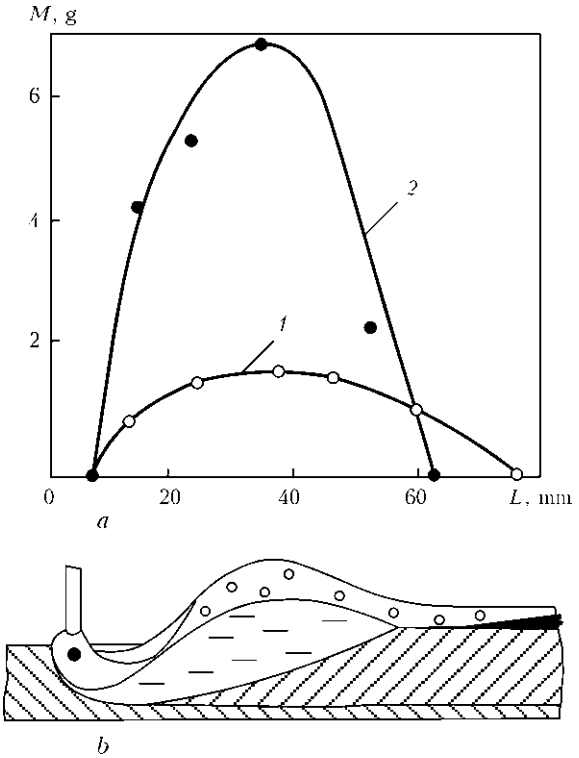

Figure 5. Curves of distribution of mass *M* of liquid slag (*1*) and metal (*2*) along the weld pool in electric submerged-arc welding obtained by application of an improved procedure of weld pool turning over and control of object mass (*a*), and schematic of the above-mentioned process (*b*)

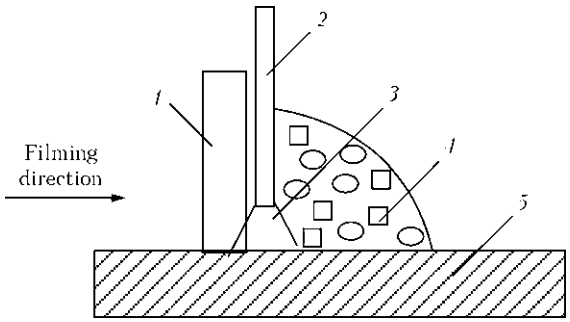

Figure 6. Schematic of an experiment on visual observation of the arcing process in electric submerged-arc welding: *1* — window glass; *2* — electrode; *3* — electric arc; *4* — flux; *5* — steel plate

In order to reveal the presence of slag bubble in electric submerged-arc welding, we conducted one more experiment. For this purpose individual beads were deposited on plates, in which a gradual starting from 25 mm (complete shielding of the arc), and then millimetre by millimetre lowering of flux pouring level was performed. All the experiment stages were recorded by a video camera. It was supposed that at a certain level of flux pouring it will be possible to see the pulsing cupola of the slag bubble. However, despite the monotonic lowering of the flux layer thickness, it was not possible to capture this moment in the filmed video material. Just baring of the arc without slag bubble formation and, vice versa, sagging of flux portion in the arcing zone were observed. The flux sagging was caused by formation of a crater in the metal, reduction of flux volume in melting and slag ejection by the arc towards weld pool tail part.

To provide a more convincing confirmation of slag bubble absence, we developed a procedure that enables visual observation of the arcing zone directly during electric submerged-arc welding (Figure 6). Here, window glass was used as a transparent screen and slag-forming material at the same time. The procedure was developed, taking into account the main postulates of our earlier thermophysical and hydrodynamic investigations. Here two alternative points of view were assessed. According to the first one, if formation of the gas bubble occurs during welding, then glass melting, formation of a shell around the arc from the glass melt and its shielding, respectively, take place. In the opposite case, glass melts in the post-arc space, no arc shielding occurs, and the arc can be observed directly. Results of experiments in the form of arcing phases successive in time in electric submerged-arc welding, are given in Figure 7. Studying the filmed material led to the conclusion that no arc shielding occurs during welding, the arc is clearly visible during the entire welding process, and no slag bubble forms around it. Liquid slag does not rise above the running arc level, but is concentrated on weld pool surface. This is readily visible in Figure 7 by the bright strip (tail) of hot slag in the post-crater zone of weld pool. This confirms the absence of slag shielding of weld pool crater zone and the essential role of gas shielding. At the same

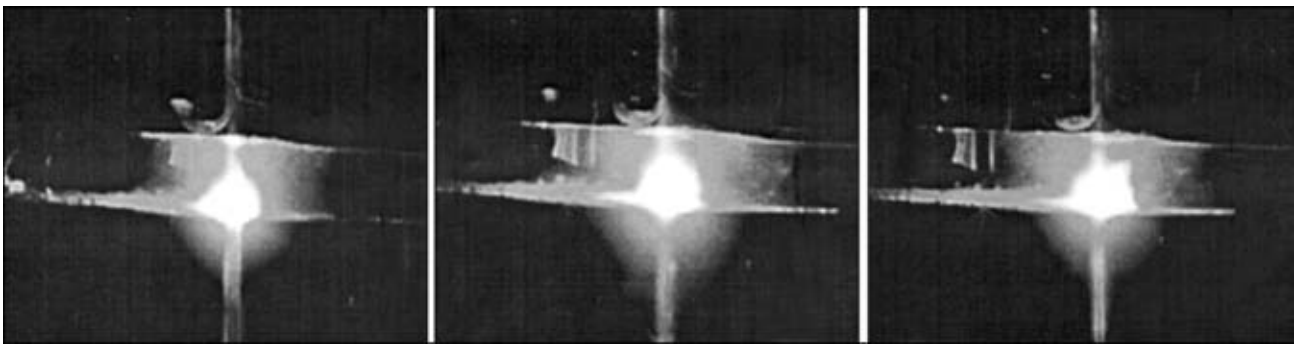

Figure 7. Three successive fragments of arcing phases in electric submerged-arc welding obtained in an experiment (see Figure 6) when welding process runs from left to right

time, the above circumstance became the subject of discussion [35–37] and were the basis for development by us of a new class of surface-fluorinated welding fluxes with 0.5–3.0 wt.% fluorine content in the surface layer of their grains. Such fluxes, even porous and of basic type, have a low susceptibility to hydratation, high resistance to weld metal porosity because of rust and improved sanitary-hygienic characteristics in welding [38–40].

To obtain a complete picture of the process of electric submerged-arc welding, we studied the features of cooling and solidification of welding slag in the post-arc zone [3]. Unlike the generally accepted schematic of the welding process (see Figure 1), availability of an extended region of liquid condition of slag is established, which goes far beyond the weld pool limits. These data were obtained as a result of application of the traditional procedure of weld pool turnover [3]. High heat-insulating properties of slag have a great influence on the cooling rate and configuration of the zones of solidified and liquid slag. In this case, mostly heat removal into the metal takes place that is related to a change of the temperature field due to displacement of the electric arc along the weld axis. Here the slag solidifies, first of all in those points on weld metal surface, where its temperature decreases to slag melting temperature. In the direction away from the arc, further gradual lowering of temperature and monotonic increase of thickness of solidifying slag take place with separation and thermal insulation of the tail located above the liquid slag volume. A new schematic of the process of electric submerged-arc welding, taking into account the features of slag cooling down in the post-arc zone given in Figure 8, provides an explanation for the earlier unconsidered mechanism of flux solidification in electric arc welding. A considerable mass of overheated slowly cooling slag above the weld pool acts as its thermal extension that increases the length of time of weld metal staying in the liquid state and promotes its degassing. A large volume of liquid slag above the solidifying and solidified metal is a cavity that absorbs the gases evolving from the weld metal. Owing to presence of an elastic wedge-like film of slag on the surface of solidifying weld metal, it is possible to apply in electric submerged-arc welding fluxes with a higher melting temperature than that of the metal being welded. This also accounts sometimes for porosity formation in the lower part of the slag crust at intensive gas evolution

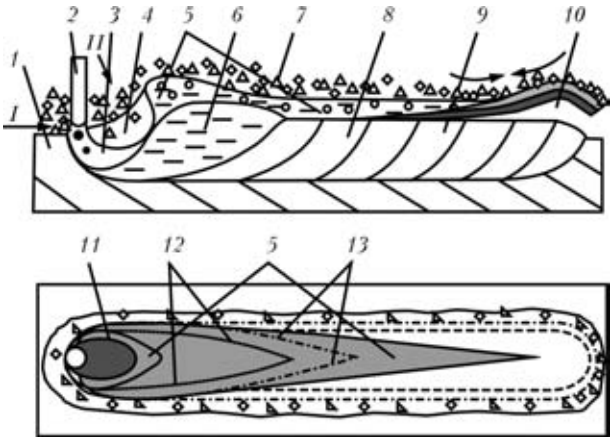

Figure 8. Precised schematic of the process of electric submerged-arc welding: *1* — base metal; *2* — electrode metal; *3* — arc plume; *4* — crater; *5* — liquid slag and its extended tail; *6* — weld pool; *7* — flux; *8* — weld; *9* — glass-like, wedge-like solidifying slag layer; *10* — crystalline layer of solidifying slag; *11* — crater zone not covered by liquid slag; *12*, *13* — line of melting isotherm of flux and slag, respectively; *I*, *II* — ways of flux penetration into the arc

from the metal that does not come to its surface. Differences in the rates of cooling of slag layer adjacent to the weld and above-lying layer lead to essential differences in their structure. Slag layer contacting the weld surface cools down faster and forms a glass-like structure, whereas the above-lying slag layer is completely or partially solidified, owing to its thermal insulation. It has a much greater coefficient of thermal compression than that of glass-like slag layer, leading to bending of this two-layer structure, and is spontaneous separation from the cooling weld (see Figure 8). Such a mechanism of slag crust separability is particularly effective, when high-silicon welding fluxes are used.

CONCLUSIONS

1. Procedure of X-ray examination of the arcing zone in electric submerged-arc welding used in works [5, 6], does not give sufficient grounds to confirm the fact of existence of a slag shell around the arc, particularly in the pre-arc zone.

2. Use of general equation of heat conductivity and Fourier law as applied to unidimensional problem in calculations of the rate of heat transfer from the arc through the shell to pre-arc zone flux, depending

on slag thermophysical characteristics, temperature gradient and thickness of slag bubble shell showed that the speed of shell restoration (speed of shifting of flux melting isotherm) is by 3–4 orders of magnitude lower than the real welding speed.

3. As a result of an extremely low speed of restoration of the shell pre-arc component, no flux melting through formation of a slag bubble occurs in electric arc welding. Under the real welding conditions, the arc rolls over the flux, entraps it and melts it under the impact of its own gas-plasma flows in the convective mode more effective in terms of energy.

4. Configuration of the zones of solidified and liquid slag in the post-arc zone and their temperature in electric submerged-arc welding are determined by heat removal into the metal, and owing to high thermally insulating properties of the flux, they are accompanied by formation of an extended liquid slag tail, separated from the weld metal by a wedge-like layer of solidifying slag crust.

5. Change of slag cooling rate leads to formation of a two-layer structure of the slag crust (glass-like — near the weld, and crystalline — higher up). At its further cooling the differences in the values of the coefficient of thermal compression lead to bending of the slag crust that promotes its separability from the weld metal.

1. Kuzmenko, V.G. (1998) About continuity of slag shell in submerged-arc welding. *Avtomatich. Svarka*, **3**, 14–19.
2. Kuzmenko, V.G. (2000) On the features of flux melting in electric arc welding. *The Paton Welding J.*, **11**, 57–58.
3. Kuzmenko, V.G. (1999) Features of melting and solidification of flux in electric arc welding. *Svarochn. Proizvodstvo*, **10**, 16–22.
4. Badianov, B.N. (1999) New scheme of submerged-arc welding process. *Ibid.*, **6**, 18–29.
5. Ostapenko, N.G., Medovar, B.I. (1947) X-ray analysis of submerged arc zone. *Avtogennoe Delo*, **11**, 16–20.
6. Grebelnik, P.G. (1950) X-ray analysis of automatic submerged-arc welding process. *Avtomatich. Svarka*, **6**, 18–29.
7. Pokhodnya, I.K. (1964) Method of analysis of electrode melting and transport process in welding. *Ibid.*, **2**, 1–10.
8. Gobarev, L.A., Mazel, A.G., Shmeleva, I.A. et al. (1973) Analysis of submerged arc in welding using pulse X-ray apparatus. *Ibid.*, **2**, 69–70.
9. Eichhorn, F., Dilthey, U. (1971) High-speed X-ray photography for submerged arc welding. *Metal Construction and British Welding J.*, 3(**12**), 453–456.
10. Kasatkin, A.G. (1973) *Processes and apparatuses of chemical technology*. Moscow: Khimiya.
11. Kuehling, H. (1982) *Reference book on physics*. Moscow: Mir.
12. Rykalin, N.N. (1951) *Calculations of thermal processes in welding*. Moscow: Mashgiz.
13. Litovsky, E.Ya., Puchkelevich, N.A. (1982) *Thermophysical properties of refractory materials*. Moscow: Metallurgiya.
14. Krzhizhanovsky, R.E., Shtern, Z.Yu. (1973) *Thermophysical properties of inorganic materials*. Leningrad: Energiya.
15. Misnar, A. (1968) *Heat conductivity of solids, liquids, gases and their compositions*. Moscow: Mir.
16. Chekhovsky, V.Ya., Ulashchik, A.N. (1987) Heat conductivity of slags in solid and molten states. *Teplofizika Vys. Temperatur*, 5(**5**), 924–928.
17. Yavojsky, Ya.I. (1967) *Theory of steelmaking processes*. Moscow: Metallurgiya.
18. (1964) *Steelmaking*. Vol. 1. Moscow: Metallurgiya.
19. Sakura, T., Emi, T., Ohata, H. et al. (1982) Determination of heat conductivity of slag melts by modified method of laser beam. *Nihon Kinzoku Gakkaisha*, 46(**12**), 1131–1138.
20. Egorov, V.N., Kondratenkov, V.I., Kilesso, V.S. (1972) Thermophysical properties of some glasses and pyroceramics. *Teplofizika Vys. Temperatur*, **5**, 95–99.
21. Serebrennikov, N.I., Geld, P.V. (1968) Enthalpy and temperature of slag melting in aluminothermic fabrication of some ferroalloys. *Izvestiya Vuzov. Series Tsvet. Metallurgiya*, **4**, 39–44.
22. Maurakh, M.A., Mitin, B.S. (1979) *Liquid refractory oxides*. Moscow: Metallurgiya.
23. Vajsburd, S.E., Zedina, I.N. (1970) Thermal properties of some silicates in liquid state. In: *Physical chemistry of molten slags*. Kiev: Naukova Dumka.
24. Bobylev, I.B., Anfilogov, V.N. (1983) Method of calculation of molten slag density. *Metally*, **4**, 37–44.
25. Erokhin, A.A. (1979) Force effect of arc on molten metal. *Avtomatich. Svarka*, **7**, 21–26.
26. Chigarev, V.V., Shchetinin, S.V. (2001) Distribution of welding arc pressure. *The Paton Welding J.*, **9**, 8–11.
27. Suzdalev, I.V., Yavno, E.I. (1981) Device for analysis of nature of distribution of welding arc force effect. *Svarochn. Proizvodstvo*, **3**, 37–38.
28. Kovalev, I.M., Krichevsky, E.M., Lvov, V.N. (1974) Effect of metal motion in welding pool on arc stability and weld formation. *Ibid.*, **11**, 5–7.
29. Mechev, V.S. (1983) Welding arc pressure on molten metal. *Ibid.*, **9**, 8–10.
30. Potekhin, V.P. (1986) Role of welding arc pressure in formation of undercuts. *Ibid.*, **8**, 38–39.
31. Wieneke, R. (1957) Ueber physikalische Vorgange in Lichtbogen. *Schweissen und Schneiden*, 9(**9**), 428–434.
32. Petrunichev, V.A. (1958) Pressure of high power arc on welding pool. *Ibid.*, **7**, 14–17.
33. Leskov, G.I. (1970) *Electric welding arc*. Moscow: Mashinostroenie.
34. Nebylitsyn, L.E., Lenivkin, V.A., Dyurgerov, N.G. (1976) Determination of parameters of plasma jet in consumable electrode welding. *Avtomatich. Svarka*, **2**, 8–10.
35. Lyubavsky, K.V., Timofeev, M.M. (1951) Influence of variation of high-manganese flux composition on its properties. *Avtogennoe Delo*, **6**, 5–9.
36. Kirdo, I.V., Podgaetsky, V.V. (1949) On effect of fluxes on porosity of automatic weld caused by rust. *Trudy po Avtomatich. Svarke pod Flyusom*, **6**, 36–62.
37. Podgaetsky, V.V., Novikova, T.P. (1960) On emission of silicon fluoride in heating of flux during welding and drying. *Avtomatich. Svarka*, **6**, 19–22.
38. Kuzmenko, V.G., Guzej, V.I. (2004) Hydration of fluxes with a locally-changed chemical composition of grains. *The Paton Welding J.*, **6**, 41–43.
39. Kuzmenko, V.G., Guzej, V.I. (2005) Pore formation in weld metal in submerged arc welding with surface saturation of grains with fluorine. *Ibid.*, **2**, 14–17.
40. Kuzmenko, V.G., Guzej, V.I. (2006) Sanitarian-hygienic characteristics of welding fluxes with locally-changed chemical composition of grains. *Ibid.*, **2**, 37–39.